International Journal of GEOMATE, Jan., 2025 Vol.28, Issue 125, pp.1-10
ISSN: 2186-2982 (P), 2186-2990 (O), Japan, DOI: https://doi.org/10.21660/2025.125.4598
Geotechnique, Construction Materials and Environment

# PREDICTING THE EFFECT OF BED MATERIAL SIZE AND GEOGRID ON LOCAL SCOUR AROUND THE BRIDGE PIER IN CLEAR WATER FLOW CONDITIONS

*Deepak Negi[1], Aarati Baral Gautam[2] and Uchimura Taro[3]

[1, 2 & 3] Graduate School of Science and Engineering, Saitama University, Japan

*Corresponding Author, Received: 21 June 2024, Revised: 23 September 2024, Accepted: 29 September 2024

**ABSTRACT:** The flow-structure-soil interaction around bridge piers results in an unwanted phenomenon called local scouring. Past evidence shows that local scours are the dominant cause of the bridge pier failures. Equilibrium scour depth in a local scour is the function of the bed material, fluid, and obstruction parameters. This paper presents the effect of the mean size of bed material ($D_{50}$) on local scour and by choosing the appropriate bed material, the effect of geogrid on local scour was assessed in a clear-water flow condition. Geogrid, having a good capacity for soil reinforcement and stabilization, a high lifetime, low environmental problems, and low cost, has not yet been used to control local scours. So, phase-I of the experiment was conducted in silica sand no. 4 and 5 without using geogrid (Non-Geogrid Case-NG), and the corresponding equilibrium scour hole parameters $S_d$, $S_l$, and $S_w$ ($S_d$, $S_l$, and $S_w$ are equilibrium depth, length, and width of scour hole respectively) were recorded. In phase-II, geogrid having hexagonal aperture shape with aperture size 4mm×2mm (8 times $D_{50}$) were used at different placement depths to cover the entire $S_d$, $S_l$, and $S_w$ obtained in NG-case. The results showed that the scour hole parameters $S_d$, $S_l$, and $S_w$ were found more prominent in silica sand no. 5 than in sand no. 4. Compared to higher placement depths, geogrid was found to be more effective at lower placement depths with maximum efficiency of 67.86% scour reduction at placement depth of 0.2 times $S_d$. Furthermore, at placement depths equal to or more than $S_d$, geogrid did not affect local scour.

*Keywords: Local scour, Equilibrium scour depth, Equilibrium scour length, Equilibrium scour width, Geogrid*

## 1. INTRODUCTION

Bridge failures are quite common events that happen across the world every year. There may be several causes of such failures, but prominent of them is the local scour. The local scour around the bridge pier accounts for around 60% of all bridge failures globally [1]. Simply, local scour is the removal of bed sediments from around the hydraulic structures when such structures are subjected to water flow. This phenomenon ultimately decreases the effective depth of bridge piers and can cause tilting and buckling failures [2], thereby resulting in a huge loss of life and capital without warning [3]. Thus, local scours are considered a major problem in hydraulic and geotechnical engineering.

The horse-shoe and wake vortices generated at the upstream and remaining soil-structure interface are responsible for forming a scour hole at the base of the pier. Whenever the water flow in a channel is obstructed by any physical obstructions like a pier, the three-dimensional flow separation called boundary layer separation takes place. A stagnation point with almost nil approach velocity is formed at just the upstream face of the obstruction, with a slight increase in the flow level as well. Due to this stagnation, the water pressure is increased at the upstream face of the pier forming a vertical pressure gradient in the upstream face, resulting in the downward flow separation. The downward flow of water in the upstream face hits the bed soil and rolls up forming a characteristic shape of the shoes of the horse, called Horse-shoe vortices. Whenever the shear stress of these vortices exceeds the shear strength of the bed soil, sediments begin to transfer from around the pier's base, forming the local scour hole. The strength of the horse-shoe vortices gets reduced when the depth of the scour hole increases. As the scour hole attains maximum depth, the strength of the horseshoe vortices decreases, and once the shear stress exerted by the flow is less than the critical shear stress of the soil, maximum depth is achieved [4]. Similarly, the flow separation along either side of the pier, on converging just downstream of the pier generates wake vortices too. These vortices rotate along the vertical axis and take up sediments like a vacuum pump and carry away from the pier's surroundings. The periodic shedding of the wake vortices leads to the transportation of sediment particles, which are deposited at some distance behind the pier [5], forming the deposition called dunes. The local scour process is thus a complex process that is affected by several parameters related to flow characteristics, bed sediment characteristics, pier geometry characteristics, and time [6].

As the local scour process ultimately leads to the bridge foundation failure, it is a matter of concern for geotechnical engineers to address the problem. Several studies have been done to control the local scour by using measures that restrict the flow-

structure interaction and the flow-soil interaction. The major concern about these measures is the cost-effectiveness, ease of construction, installation, and maintenance. The erosive action of horseshoe and wake vortices can be significantly reduced, If one can stabilize and reinforce the bed soil around bridge piers by using geosynthetic materials. In recent decades, with the leapfrog development in polymer science, geosynthetic materials were found to have high life, cost-effectiveness, and environment-friendly measures for soil reinforcement and stabilization [7]. Ghassemi et al., 2016 conducted a laboratory experiment to study the effectiveness of geonet in reducing scour downstream of the stilling basin [8]. The effect of geonet on local scouring showed that if the placement depth of the geonet is lower than the maximum scour depth at equilibrium and without geonet states, the maximum scour depth and volume of the scour hole decrease, and the maximum length of the scour hole will increase. Abbas & Tanaka, 2022 in their study utilized the pooled water depth and geogrids of different aperture sizes (G1=6.5 mm & G2=2.5 mm), separately and in combination, to reduce scouring on the downstream side of a levee [9]. They concluded that the combination of the geogrids and pooled water played a vital role in suppressing the scour depth. The performance of the G1M (Geogrids-1 & Mobile bed) case was found to be more effective as compared to NM (Nothing & Mobile bed) with approximately 57-78% scour reduction. Furthermore, the performance of the G2M (Geogrids-2 & Mobile bed) case was found to be more effective as compared to G1M & NM cases (Nothing & Mobile bed) with 100% scour reduction.

This study aims to predict the effectiveness of geogrid in controlling local scour around bridge piers. The placement depths of geogrid were determined based on the scour parameters obtained in the non-geogrid case and the effect of geogrid at different placement depths was measured in terms of percentage efficiency of maximum scour reduction as compared to the non-geogrid case.

## 2. RESEARCH SIGNIFICANCE

The applicability and suitability of geosynthetic material in controlling local scour around the bridge pier have not been assessed till now. So, this model study was conducted to analyze the effect of geogrid on local scour around the bridge pier for a given discharge in clear water flow conditions. The results of this study are expected to be helpful for better understanding and utilization of geosynthetic materials for the stability of bridge foundations.

## 3. MATERIALS AND METHODS

### 3.1 Experimental Setup

The experiment was conducted in the Geotechnical and Geosphere Laboratory of Saitama University. The test model consisted of a re-circulating rectangular flume having 2 m length (L), 0.20 m breadth (B), and 0.20 m height (H). The material of the flume was transparent acrylic made to facilitate the experimental observations. The submersible pump was inserted into the downstream reservoir (capacity 120 liters) to feed the water into the flume through the upstream reservoir (capacity 140 liters). The total flume length was divided into three (3) sections: An upstream section of 0.5 m length, a working section of 1.10 m length, and a downstream section of 0.4 m length. The working section of the flume was filled with the testing silica sand, whereas the upstream and downstream sections were made rigid using wooden false beds to minimize the effect of turbulence generated at the upstream end due to the inlet reservoir and to avoid the backwater effect due to gate closing at the downstream end of the flume. Furthermore, a honeycomb baffle structure and perforated gradual reducer were used in the upstream inlet reservoir to ensure smooth flow into the flume. A hand-operating tailgate was inserted at the end of the flume to maintain the required flow depth, and a flowmeter and control valve were used to control the required discharge in the flume channel. The pier models were inserted at 1.2m from the upstream end, and at the middle of the flume width to minimize the effect of inlet disturbances and tailgate. The laser meter was used to level the bed sediments before and after each run. The equilibrium scour images were recorded by using a depth camera (Intel real sense D435) from the top and the scour initiation and development process was recorded by digital camera from the sides. The schematic plan and side view of the model apparatus are shown in Fig. 1.

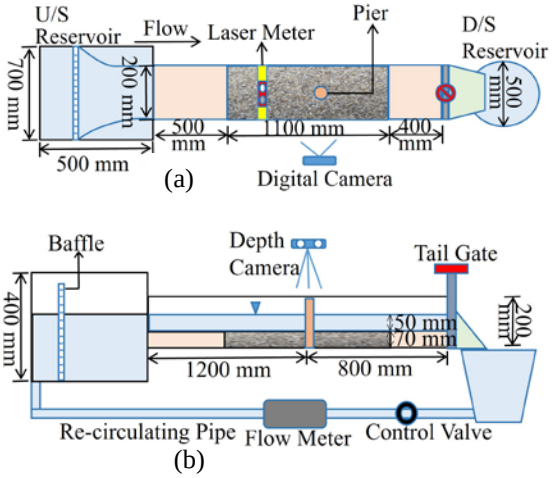


Fig. 1 Schematic details of Experimental Setup: (a) Plan; (b) Side View

### 3.2 Parameter Selection

In this study, uniform silica sand no. 4 and 5, having density of 2.65 gm/cc with average particle size (D50) of 0.96 mm and 0.49 mm, respectively, were used. Silica sand was selected to avoid ripple formation during the experiment, which was as per ref. [10] recommendations. The wooden circular pier with a diameter of 2 cm was used for the experiment. A circular-shaped pier was selected, being mostly found shape in real fields, and the size of the pier was selected so as not to exceed 10% of the flume width, to avoid the flume wall effect on scour rate as per ref. [11] recommendations. To obtain the maximum scour depth in clear-water conditions, experiments were performed using uniform sediment ($C_u \leq 2$) with flow-intensity values slightly less than the threshold condition of sediment movement ($0.9<V/V_c<1$) as suggested by ref. [12], where V is the mean flow velocity of water and $V_c$ is the critical velocity of bed sand. The critical velocity of bed sand ($V_c$) was calculated by averaging the data obtained from visual observation as suggested by Kramer, and the theoretical critical velocity of bed soil was calculated based on ref. [13] recommendations. The mean flow velocity (V) for each run of the tests was taken as 0.95 times $V_c$, whereas the flow depth (y) was maintained as 5 cm as per ref. [14] suggestions. Also, the model parameters were scaled down at 1:30 from the original prototypes.

### 3.3 Geogrid Properties and Functioning

Solid rib bi-axial geogrid made from highly dense polyvinyl chloride was used. A geogrid of hexagonal-shaped apertures was chosen. The size of the apertures was related to the mean size of the bed material ($D_{50}$) and the aperture size of 8 times $D_{50}$ was considered. Based on laboratory measurements, the physical and mechanical properties of the geogrid used in this study are presented in Table 1.

Geogrid was expected to control local scour by interlocking the bed particles and stabilize the bed sand by holding and capturing the bed particles together. Particle-to-particle interaction makes bulk effect to form a single large particle size for holding and capturing functions. Apertures in geogrid help to interlock the bed particles together and prevent upliftment due to the pumping action of wake vortices (WVs). Furthermore, shear stress by horse-shoe vortices (HSVs) on bed soil results in lateral movement and upliftment of bed particles as well.

The geogrid layer, which possesses sufficient frictional resistance (due to tension) acts as a restrainer against lateral movement and upliftment and as well as opposes lateral movement of bed particles below it.

Table 1. Physical and Mechanical Properties of the Geogrids used in this Study

| Property | Value/Description |
|---|---|
| Mass per Unit Area ($g/m^2$) | 350 |
| Tensile Stiffness (KN/m) | 59 |
| Aperture size (mm) | 4×2 |
| Aperture Shape | Hexagonal |
| Nominal Thickness (mm) | 1 |
| Chemical Resistance | High |

### 3.4 Study Phases

The experiments were conducted in two phases. Phase I consisted of non-geogrid cases, in which local scour tests were done in two different silica sands (Sand no. 4 and 5). Based on the nature of scour hole parameters ($S_d$, $S_l$, and $S_w$) in phase I, phase II experiments using geogrid were done to find the effect of geogrid at different placement depths.

#### *3.4.1 Phase-I: Non-Geogrid (NG) Cases*

Non-geogrid cases were designated as NG cases, silica sand no. 4 as S4, and silica sand no. 5 as S5. Local scour tests were conducted separately on silica sands S4 and S5 without using geogrid. An incipient condition test on S5 was done to calculate the practical critical velocity, which was then averaged with theoretical, critical velocity to get an average critical velocity of bed sand ($V_c$) as 35.9 cm/s. By adopting the flow intensity ($I=V/V_c$) value of 0.95, the mean flow discharge during the experiment was maintained at 3.41 liter per second by using a control valve and flowmeter. Equilibrium scour time ($T_s$) was fixed by conducting the temporal variation test on S5. The scour hole obtained after each experimental run was recorded by Depth camera and the depth images were then analyzed using cloud compare software to obtain scour hole parameters $S_d$, $S_l$, and $S_w$ and dune height ($H_d$), which were then used to study the effect of bed material mean size ($D_{50}$) on local scour. Phase I consisted of the cases as shown in Table 2.

Table 2. Non-Geogrid (NG) Experimental cases

| No. of Cases | Bed Sand | Non-Geogrids Case | Case Designation | Remarks |
|---|---|---|---|---|
| 1 | S5 | NG | S5-NG | Phase-I |
| 2 | S4 | NG | S4-NG | |

*3.4.2 Phase-II: Geogrid (G) Cases*

Geogrids cases were designated as G cases. As the scour hole parameters like $S_d$, $S_l$, and $S_w$ were found more distinct and prominent in S5, the Geogrid cases were conducted in S5. Each experimental run was conducted by placing the geogrid at an interval of 0.2 times $S_d$ (i.e., at each 20% of equilibrium scour depth in NG Case) from the bed surface along varying placement depths to cover the entire $S_d$ of the NG-cases. Geogrid was also placed to cover the entire length and width of the scour hole in the plan view. For this purpose, geogrid was extended to half the pier diameter (D/2) in both the length and width side of the scour hole, and its edges were fixed to the bed soil with anchoring pins, so that it could not move due to the fluctuations of the flow during the experiments. Then, some sediments were poured over the geogrid until the sediment surface was leveled before having the test run. The installation method of Geogrid is shown in Fig. 2.

The scour holes generated after each experimental run of 3 hours were recorded again by using a Depth camera and the depth images were analyzed to calculate $S_d$, $S_l$ and $S_w$ in each Geogrid (G) case. The effectiveness of geogrid at different placement depths was then calculated by using formula (1).

$$\text{Percentage reduction (\%)} = [(S_d)_{NG} - (S_d)_G] *100/(S_d)_{NG} \quad \ldots\ldots\ldots\ldots\ldots\ldots\ldots\ldots\ldots\ldots (1)$$

Where $(S_d)_{NG}$ is the equilibrium scour depth in silica sand no. 5 without using geogrid in NG case and $(S_d)_G$ is the equilibrium scour depth in silica sand no. 5 using geogrid at different placement depths in G-cases.

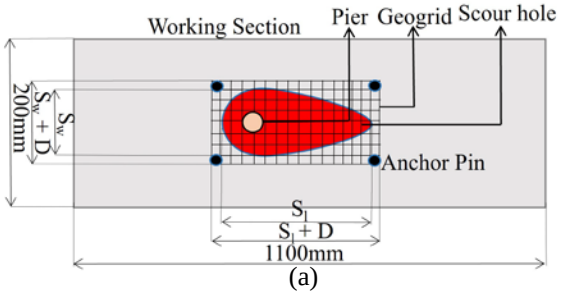


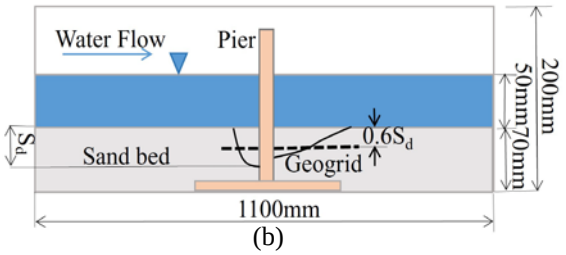


Fig. 2 Geogrids Installation (a) Plan; (b) Elevation (Geogrids installed at depth $0.6S_d$)

Phase II consisted of the experimental cases with geogrid placed at different placement depths as shown in Table 3. The case designation 0Sd to 1.1Sd represents the geogrid placed at the bed surface to the geogrid placed at 110% of equilibrium scour depth (of NG case) from the bed surface.

## 4. RESULTS AND DISCUSSIONS

### 4.1 Non-Geogrid (NG) Case Results and Analysis

From incipient condition test and theoretical calculations, the critical velocity of bed sand ($V_c$) was fixed 35.9 cm/s. Fig. 3 shows the results of time variation of scour up to 270 minutes. From the graph, it can be retrieved that there was rapid scour development during initial phase and almost 78% of the equilibrium scour depth was attained within first 30 minutes. Result also shows that after 3 hours (180 minutes) to 4.5 hours (270 minutes), there was only 0.18% increase in the scour depth. It was seen that the scour process initiated from the downstream part of the pier-sand interface and gradually progressed towards the upstream through the either side to form rapid turbulence of bed particles and ultimately the scour hole developed rapidly in all three dimensions. The rapid development of scour hole during initial phase was due to the higher strength of horseshoe and wake vortices at relatively shallower depth of scour hole. As the depth of the scour hole increased, the strength of both the vortices diminished and the process became milder and ultimately the increase in scour depth became negligible after 3 hours of the experiment.

Table 3. Geogrid (G) Experimental cases

| No. of Cases | Bed Sand | Geogrids Case | Placement Depth of Geogrids (From bed surface) | Case Designation | Remarks |
|---|---|---|---|---|---|
| 1 | S5 | G | 0Sd | S5-G-0Sd | Phase-II |
| 2 | S5 | G | 0.2Sd | S5-G-0.2Sd | |
| 3 | S5 | G | 0.4Sd | S5-G-0.4Sd | |
| 4 | S5 | G | 0.6Sd | S5-G-0.6Sd | |
| 5 | S5 | G | 0.8Sd | S5-G-0.8Sd | |
| 6 | S5 | G | 1Sd | S5-G-1Sd | |
| 7 | S5 | G | 1.1Sd | S5-G-1.1Sd | |

As the scour process was negligible after 3 hours, 3 hours was taken as the equilibrium experimental time for all the cases.

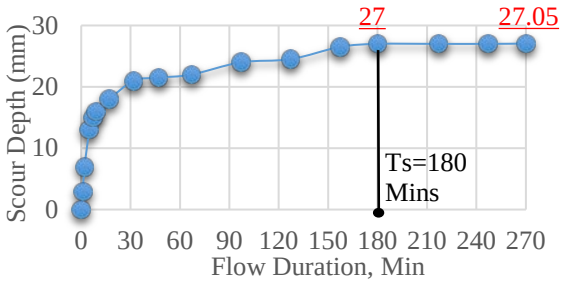


Fig. 3 (a) Time variation of scour (at I=0.95 and Q=3.41Lps)

After fixing the equilibrium scour time ($T_s$) from the time variation of the scour test, Non-geogrid (NG) cases were done at flow intensity ($I=V/V_c$) of 0.95 and Q=3.41 lps. The results after 3 hours of the control experimental run are shown in Table 4.

Table 4. Non-Geogrid (NG) cases result

| Case Name | $S_d$ (mm) | $S_l$ (mm) | $S_w$ (mm) | $H_d$ (mm) |
|---|---|---|---|---|
| S5-NG | 28 | 96 | 106 | 24 |
| S4-NG | 13 | 52 | 60 | 9 |

The equilibrium scour depth ($S_d$) in both cases is the maximum scour depth observed around the base of the pier. As the base of the pier below the ground surface was graduated along all four sides to measure the equilibrium scour depth reading near the pier's surface, the higher value of the scour depth readings obtained from the depth camera and graduated tape was recorded as the equilibrium scour depth ($S_d$). The remaining scour hole parameters $S_l$, $S_w$, and dune height ($H_d$) were obtained from the depth camera readings. From the data results in Table 4, it can be seen that the scour hole parameters and dune height are significantly prominent in S5 compared to S4. Because of the higher unit weight of individual sand particles in S4, these particles have less tendency to uplift, erode, and roll up with the same magnitude of horseshoe and wake vortices compared to S5. Furthermore, S5 particles are more uniform than S4 particles, and the inter-particle bonding for lateral shear resistance is weaker in silica sand 5 (S5). Thus, the weaker lateral shear resistance due to the lower value of $C_u$ and lower unit weight of individual sand particles of silica sand 5 (S5), particles are responsible for significantly higher values of $S_d$, $S_l$, and $S_w$ compared to silica sand 4 (S4). Since the dune volume and dune height have a direct proportional relation with scour hole parameters, the higher value of dune height ($H_d$) in silica sand 5 (S5) is justifiable.

Fig. 4 represents the comparative profile and cross-section of the scour hole along the maximum scour depth point obtained from depth image analysis.

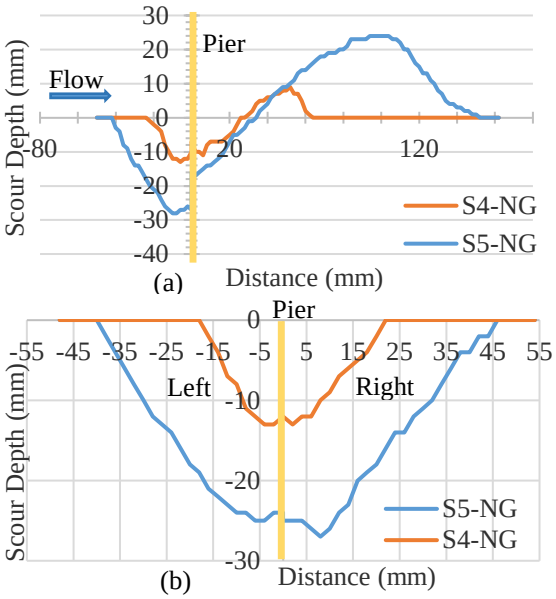


Fig. 4 (a) Comparison of Profile between S4-NG and S5-NG case (b) Cross-section comparison between S4-NG and S5-NG case

Fig. 4 (a) shows an equilibrium scour depth ($S_d$) of 13 mm at 6 mm upstream from the upstream face of a pier in the S4-NG case, whereas it was 28 mm in the S5-NG case and located at 8 mm upstream from the upstream face of the pier. Equilibrium scour depth values ($S_d$) obtained from the depth image were higher than graduated tape readings in both cases. Fig. 5 shows the graduated tape readings and normal and depth images of the experimental cases.

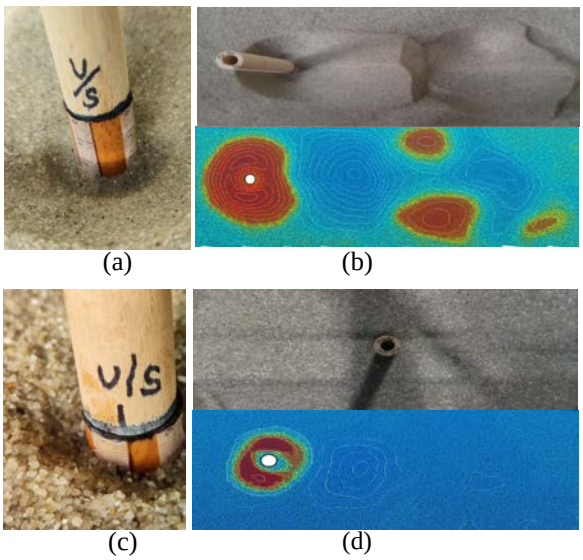


Fig. 5 (a) Graduated tape reading (S5-NG case), (b) Normal and Depth Image of scour hole (S5-NG case), (c) Graduated tape reading (S4-NG case), (d) Normal and Depth Image of scour hole (S4-NG case)

### 4.2 Geogrid (G) Case Results and Analysis

As the scour hole parameters were significantly prominent in silica sand 5 compared to silica sand 4, the effectiveness of geogrid was studied in silica sand 5 by placing it at different placement depths. When the experimental run was conducted by placing geogrid at the sand bed surface (S5-G-0Sd Case), geogrid was uplifted due to horse-shoe eddies and the buoyant force of water. Though the geogrid was fixed at all the ends by anchor pins, it uplifted within the first 5 minutes of the experimental run and did not serve its function. The experiments were continued for other placement depths and the result is tabulated in Table 5. The placement depths of geogrid were selected to cover the entire equilibrium scour depth ($S_d$) of 28 mm obtained in the S5-NG case. The results in Table 5 show that equilibrium scour depth ($S_d$) values are smaller in lower placement depths. Thus, geogrid was found more effective in lower placement depths compared to higher placement depths. At placement depth equal to and more than $S_d$, no effect of geogrid was found on local scour. The equilibrium scour length ($S_l$) of the scour hole was significantly higher at lower placement depths than at higher placement depths $S_l$ values. However, equilibrium scour width ($S_w$) at lower placement depths was found to be smaller compared to the corresponding values at higher placement depths of geogrid. Furthermore, the dune height ($H_d$) showed a similar pattern of change as of $S_d$ values with smaller dune heights at lower placement depths compared to higher placement depths.

Whenever geogrid was placed at a certain placement depth, it restricted the upward movement of sand particles below it due to the holding and capturing of particles. It is because the individual sand particles make particle-to-particle contact to form larger-sized particles causing bulk effect, there was an interlocking effect to hold the particles below the geogrid level. The upliftment of sand particles due to the horseshoe and wake vortices (WVs) was found to be well reduced by placing the geogrid at certain placement depths, resulting in significant reduction in equilibrium scour depth as shown in Fig. 6. Similarly, shear stresses exerted by the horseshoe vortices (HSVs) at the upstream, left, and right faces of the pier and the similar forces on the downstream bed due to water flow resulted in the extension of the scour hole in length and width directions. These forces were also found to be well encountered by the frictional resistance due to tension in the geogrid resulting in the decrease in the equilibrium scour width ($S_w$) at lower placement depth. Since there were water flow forces in addition to frictional resistance due to tension in the geogrid opposing the shear stresses exerted by horseshoe vortices in the upstream face of the pier, there was a significant reduction in the length of scour hole in the upstream face after placing the geogrid. However, there was only tension resistance of the geogrid to counter the shear forces of water flow in the downstream face of the pier and the fluctuations of the water flow over the geogrid caused further displacement of particles in the flow direction resulting in the overall increase in the equilibrium scour length ($S_l$) at lower placement depths. In the left and right faces of the pier, tension resistance of geogrid was found sufficient to counter the shear stresses of horseshoe vortices. Thus, the equilibrium width ($S_w$) of the scour hole was found smaller at lower placement depths. At higher placement depths, the shear stress and the upliftment effect of the horseshoe and wake vortices were diminished and thus the effect of geogrid was also not seen to be significant.

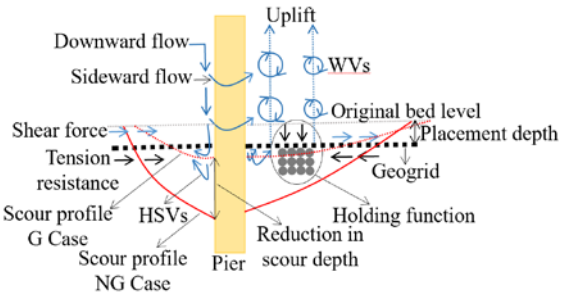


Fig. 6 Working mechanism of Geogrid to control local scour

Table 5. Geogrid (G) cases result

| Case Name | Placement depth (mm) | $S_d$ (mm) | $S_l$ (mm) | $S_w$ (mm) | $H_d$ (mm) | Remarks |
|---|---|---|---|---|---|---|
| S5-NG | | 28 | 96 | 106 | 24 | NG-case |
| S5-G-0.2Sd | 5.6 | 9 | 110 | 84 | 11 | G-Case |
| S5-G-0.4Sd | 11.2 | 13 | 106 | 86 | 16 | |
| S5-G-0.6Sd | 16.8 | 18 | 102 | 96 | 19 | |
| S5-G-0.8Sd | 22.4 | 23 | 100 | 104 | 21 | |
| S5-G-1Sd | 28 | 28 | 98 | 105 | 25 | |
| S5-G-1.1Sd | 30.8 | 28 | 96 | 107 | 25 | |

Fig. 7 shows the comparison of scour hole parameters at different placement depths of geogrid in profile and cross-section.

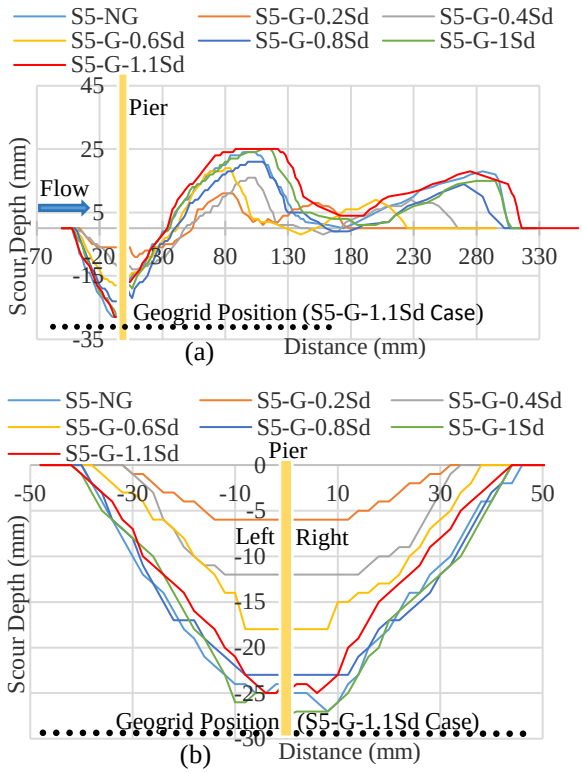


Fig. 7 (a) Comparison of Profiles of Geogrid (G) cases (b) Comparison of cross-sections of Geogrid (G) cases

It is seen that the tendency of geogrid to reduce $S_d$, $S_w$, and $H_d$ and increase $S_l$ goes on decreasing with larger placement depths of geogrid. At placement depth of $1S_d$ and more, scour hole parameters ($S_d$, $S_w$, and $S_l$) and dune parameter ($H_d$) remained unchanged with almost the same values as in Non-geogrid (NG) cases. The reason for such results might be the lower strengths of horseshoe vortices and wake vortices in generating scour holes at higher depths, and there was no effect of geogrid at higher placement depth equal to or more than $S_d$.

Fig. 8 shows geogrid installation images and after-scour images at placement depths 1Sd and 1.1Sd.

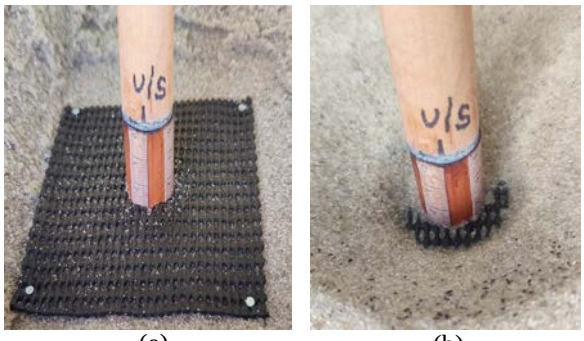


(a) (b)


(c) (d)

Fig. 8 (a) Geogrid installation at placement depth $1S_d$ (b) After scour image at placement depth $1S_d$ (c) Geogrid installation at placement depth $1.1S_d$ (d) After scour image at placement depth $1.1S_d$

The experimental results also showed the deflection of geogrid and significant scouring below it at placement depths of $0.2S_d$ and $0.4S_d$. Unlike in other cases, maximum scour depth ($S_d$) in these two cases occurred at the downstream face of the pier. The profile of scour hole and deflected geogrid is shown in Fig. 9. In both cases (S5-G-$0.2S_d$ and S5-G-$0.4S_d$), near the face of the pier, geogrid was found to be deflected downwards from its initial position. Whereas at a farther distance from the downstream face of the pier, it was found deflected upwards from its original position. Furthermore, the deflection of geogrid and scouring below it was found more prominent at a placement depth of $0.2S_d$ compared to a placement depth $0.4S_d$.

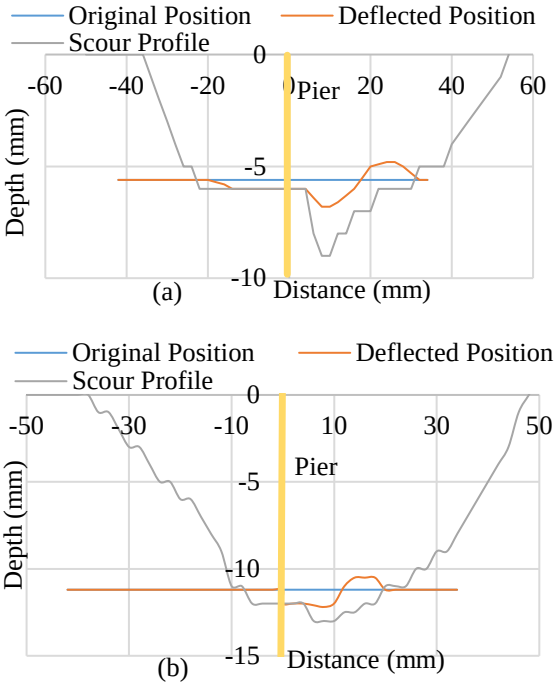


Fig. 9 Geogrid Profile (a) S5-G-$0.2S_d$ Case (b) S5-G-$0.4S_d$ Case

The deflection mechanism, after scour image and image of deflected geogrid of case S5-G-0.4$S_d$ is shown in Fig. 10. Due to the higher uplift forces of wake vortices at shallower depths and near the pier's downstream face, the sand particles tend to uplift through the apertures of geogrid at higher rate at these locations. Therefore, sand particles near the downstream face of the pier in a shallower depth of geogrid eroded and came out through apertures at a higher rate forming larger scouring below the geogrid. Once the undermining was initiated, there was rapid particle-flow interaction under the geogrid due to its armoring effect and ultimately the maximum scour depth occurred in the downstream face of the pier in S5-G-0.2$S_d$ and S5-G-0.4$S_d$ cases. Furthermore, due to the lack of support of sand particles below geogrids due to scour and larger unsupported length due to increased length of scour hole in the downstream of pier, it deflected downward from its initial position at near the downstream face of pier. Whereas, due to the flow separation below the geogrid due to the armoring effect, the sand particles moved along with flow below the geogrid towards the downstream side, and due to decreased effective area of aperture openings and bulk effect of particles, they tend to uplift the geogrids resulting in the upward deflection at a farther distance from the pier. At higher placement depths, the upliftment forces of wake vortices were not sufficiently strong enough to erode the sand particles below the geogrids.

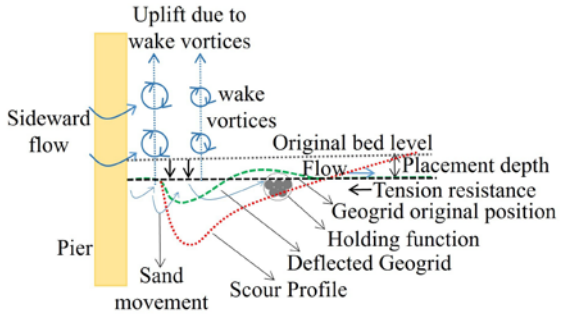


(a)

(b)

Fig. 10 (a) Deflection mechanism (b) Deflected Geogrid and After scour Image (Plan) of S5-G-0.4$S_d$ case

The relative position of maximum scour depth ($S_d$) and its extent with respect to the center of the pier along the longitudinal axis in different cases is shown in Fig. 11. Unlike other cases, maximum scour depth ($S_d$) was seen 18 mm away downstream from the center line of the pier in S5-G-0.2$S_d$ case whereas the same was seen at 16 mm downstream in S5-G-0.4$S_d$ case. Furthermore, it was seen that the extent of maximum scour depth was larger in the case of higher placement depths compared to lower placement depths of geogrid.

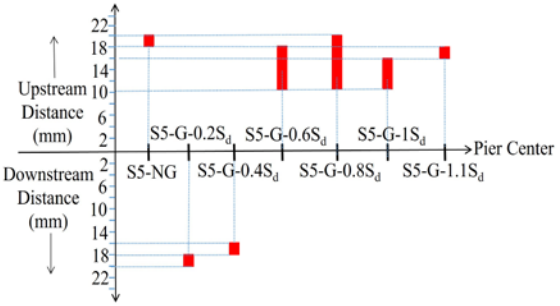


Fig. 11 Relative Position and extent of Maximum Scour depth ($S_d$)

Fig. 12 shows the variation of scour hole parameters ($S_d$, $S_l$, $S_w$) and dune height ($H_d$) in S5-NG case and different cases with geogrid installation. The figure clearly shows the incremental trend of equilibrium scour depth ($S_d$), equilibrium scour width ($S_w$), and dune height ($H_d$) with the increase in placement depth. But equilibrium scour length ($S_l$) in contrast decreases with the higher placement depths of geogrid. Furthermore, it is also seen that the scour hole parameters and dune height are almost similar in the non-geogrid (S5-NG) case, S5-G-1$S_d$, and S5-G-1.1$S_d$ cases. Thus, geogrid at placement depth equal to or more than the maximum scour depth ($S_d$) of NG case was found ineffective. The reason behind this is the reduced strength of horseshoe and wake vortices at such depths cause local scour and activate the functioning of geogrid to control the process.

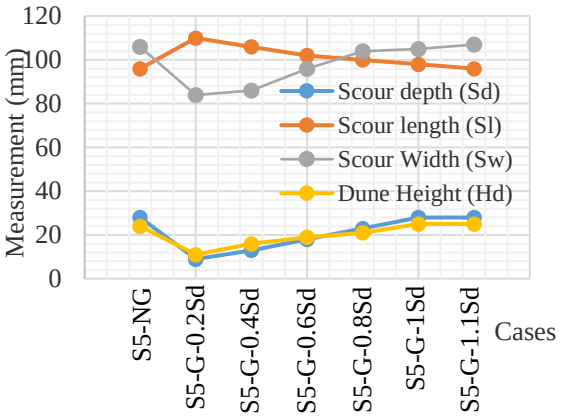


Fig. 12 Variation of scour hole and dune parameters in different cases

The scour reduction and the percentage effectiveness of different placement depths of geogrid are shown in Fig. 13. A placement depth of 0.2Sd was seen as the most effective, with 67.86% scour reduction efficiency. At placement depths of $1S_d$ and $1.1S_d$, reduction in scour depth was found to be almost nil with zero efficiency. As the geogrid placed at the bed surface did not work due to its upliftment by water flow, the case was not included in the experiment and the remaining experimental cases were conducted by providing a minimum cushion of $0.2S_d$ to cover the geogrid by sand bed material. As the scour profile did not change significantly while placing the geogrid at $1S_d$, the placement depth of $1.1S_d$ was selected to understand the effectiveness of the geogrid just below that depth of $1S_d$. The experiment showed similar results in both cases, and it is concluded that there is no meaning in installing the geogrid at depths equal to or more than the maximum scour depth of the NG case to control local scour.

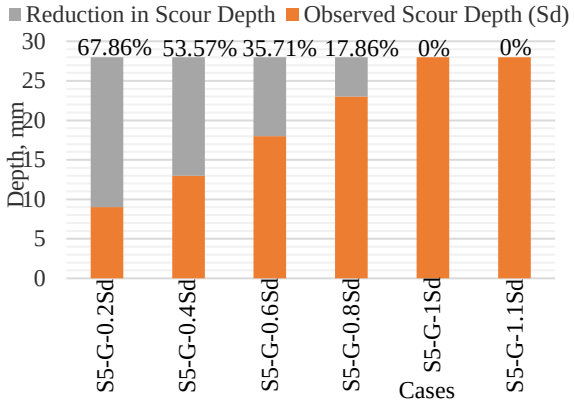


Fig. 13 Efficiencies at different placement depths of Geogrid

The results obtained in this experiment for different placement depths of geogrid are consistent with results obtained by Ghassemi et al. in their experiment to control scour by applying geonet at downstream of the stilling basin [8]. The effectiveness of the geonet at a placement depth lower than the maximum scour depth to control scour and increase in the length of the scour hole when the geonet was placed at such depths is similar with the results of this experiment. The nil efficiency of geogrid at placement depths equal to or higher than the maximum scour depth ($S_d$) of NG-case is also consistent with the conclusion made by Ghassemi et al. [8], they concluded that, when the placement depth of geonet is equal to or greater than the maximum scour depth for without geonet condition, the characteristics of scour profiles does not change. Unlike Ghassemi et al. [8] and Abbas & Tanaka [9], the deflection of geogrid was seen at lower placement depths ($0.2S_d$ and $0.4S_d$) in this experiment, for which they might not have studied the deflection of geonet and geogrid in their experiment.

From the above discussions, it can be concluded that geosynthetic materials like geogrids can reduce local scour around bridge piers. The minimum cushion depth of sand particles is needed for geogrid to prevent it from uplifting by water flow. The effectiveness of geogrid depends upon its placement depth. At lower placement depths, it is found to be more effective with maximum efficiency at the lowest placement depth of $0.2S_d$ followed by $0.4S_d$, $0.6S_d$, and $0.8S_d$. At a higher placement depth equal to or more than the maximum scour depth of NG-case, geogrid is of no effect.

## 5. CONCLUSIONS

In this research work, the effect of geogrid on local scour profiles around the single circular bridge pier was studied. For this purpose, the local scour tests were first conducted on two sand bed materials, silica sand no. 4 and 5, without using geogrid in phase I. The results of phase I were analyzed to study the effect of mean particle size on local scour. A significant and prominent scour profile obtained in silica sand no. 5 (S5-NG) was then considered as the representative case for further study. Local scour tests using geogrid (hexagonal shape, 4 mm × 2 mm aperture size) at different placement depths were done in silica sand no. 5 in phase II. Based on the experimental results, the following points can be concluded:

- For a flow condition, the scour hole and dune parameters are more significant and prominent in bed material with a smaller mean particle size and lower coefficient of uniformity.
- The existence of geogrid parallel to the bed surface at a depth less than the maximum scour depth of NG-case at equilibrium may reduce the equilibrium scour depth ($S_d$), equilibrium scour width ($S_w$), dune height ($H_d$) and increase the equilibrium length of scour hole ($S_l$).
- Geogrid has no effect on the local scour profile when it is placed at a depth equal to or more than the maximum scour depth of the NG case.
- Although geogrid deflection occurs at lower placement depths of $0.2S_d$ and $0.4S_d$, there is a significant reduction in scour depth in both cases. Furthermore, there is significant displacement of maximum scour depth location towards almost 16 to 18 mm (48 to 54 cm in prototype scale) downstream from the pier's center.

This experiment was conducted by taking a minimum cushion depth of $0.2S_d$ for geogrid, single aperture size of 8 times $D_{50}$, and aperture of hexagonal shape. So future experiments are suggested to be performed at placement depths less

than $0.2S_d$, aperture shapes other than hexagonal and aperture sizes greater and smaller than 8 times $D_{50}$.

## 6. ACKNOWLEDGEMENTS

The authors would like to acknowledge the financial support of the Japan Development Services (JDS Scholarship) under JICA and the technical support of the Department of Civil and Environmental Engineering, Geotechnical and Geosphere Laboratory of Saitama University. We also want to acknowledge the anonymous reviewers for their valuable comments on improving the manuscript and thank Er. Subodh Guragain, thank you for your continuous support during the study period.

## 7. REFERENCES

[1] Garg V., Setia B., and Verma D. V. S., Temporal variation of scour around circular bridge pier with protection device, Proceedings of Hydro International, 2013.

[2] Wardhana K., and Hadipriono F. C., Analysis of Recent Bridge Failures in the United States, Journal of Performance of Constructed Facilities, Vol. 17, Issue 3, 2003, pp. 144-150.

[3] Ahmad N., Mohammad T.A., and Suif Z., Prediction of local scour around wide bridge piers under clear-water conditions, International Journal of Geomate, Vol. 12, Issue 34, 2017, pp. 135-139.

[4] Deng L., and Cai C. S., Bridge Scour: Prediction, Modeling, Monitoring, and Countermeasures, Practice Periodical on Structural Design and Construction, Vol. 15, Issue 2, 2010, pp. 125-134.

[5] Guragain S., and Tanaka N., An Experimental Study on the Effect of Distance and Sheltering area of a Group of Linearly Arranged Sacrificial Piles on Reducing Local Scour around a Circular Bridge Pier under Clear-Water Conditions, Fluids, Vol. 9, Issue 2, 2024, pp. 35

[6] Melville B., The Physics of Local Scour at Bridge Piers, In Proceedings of the Fourth International Conference on Scour and Erosion, 2008, pp. 28-38.

[7] Touahmia M., Interaction mechanisms of soil-geosynthetic reinforcement, International Journal of Geomate, Vol. 7, Issue 13, 2014, pp. 969-973.

[8] Ghassemi A. M. I. N., Omid M. H., and Estabragh A. R., Application of geonet in reducing scour downstream stilling basin, In Proceedings of 6th Asian Regional Conference on Geosynthetics - Geosynthetics for Infrastructure Development, 2016, pp. 830-839.

[9] Abbas F. M., and Tanaka N., Utilization of Geogrid and Water Cushion to Reduce the Impact of Nappe Flow and Scouring on the Downstream Side of a Levee, Fluids, Vol. 7, Issue 9, 2022, pp. 299.

[10] Raudkivi A. J., and Ettema R., Clear-Water Scour at Cylindrical Piers, Journal of Hydraulic Engineering, Vol. 109, Issue 3, 1983, pp. 338-350.

[11] Chiew Y. M., and Melville B. W., Local scour around bridge piers, Journal of Hydraulic Research, Vol. 25, Issue 1, 1987, pp. 15–26.

[12] Melville B. W., Bridge Scour, Water Resources Publications, Vol. 112, 2000.

[13] Neill C. R., Note on initial movement of coarse uniform bed-material, Journal of Hydraulic Research, Vol. 6, Issue 2, 1968, pp. 173-176.

[14] Ettema R., Melville B. W., and Barkdoll B., Scale Effect in Pier-Scour Experiments, Journal of Hydraulic Engineering, Vol. 124, Issue 6, 1998, pp. 639-642.